JOURNAL OF BACTERIOLOGY, Dec. 2010, p. 6390–6400 Vol. 192, No. 24
0021-9193/10/$12.00 doi:10.1128/JB.00995-10

Instability of *ackA* (Acetate Kinase) Mutations and Their Effects on Acetyl Phosphate and ATP Amounts in *Streptococcus pneumoniae* D39▽†

Smirla Ramos-Montañez, Krystyna M. Kazmierczak, Kristy L. Hentchel, and Malcolm E. Winkler*

Department of Biology, Indiana University Bloomington, Bloomington, Indiana 47405

Received 22 August 2010/Accepted 4 October 2010

Acetyl phosphate (AcP) is a small-molecule metabolite that can act as a phosphoryl group donor for response regulators of two-component systems (TCSs). The serious human respiratory pathogen *Streptococcus pneumoniae* (pneumococcus) synthesizes AcP by the conventional pathway involving phosphotransacetylase and acetate kinase, encoded by *pta* and *ackA*, respectively. In addition, pneumococcus synthesizes copious amounts of AcP and hydrogen peroxide (H_2O_2) by pyruvate oxidase, which is encoded by *spxB*. To assess possible roles of AcP in pneumococcal TCS regulation and metabolism, we constructed strains with combinations of *spxB*, *pta*, and *ackA* mutations and determined their effects on ATP, AcP, and H_2O_2 production. Unexpectedly, Δ*ackA* mutants were unstable and readily accumulated primary suppressor mutations in s*pxB* or its positive regulator, *spxR*, thereby reducing H_2O_2 and AcP levels, and secondary capsule mutations in *cps2E* or *cps2C*. Δ*ackA* Δ*spxB* mutants contained half the cellular amount of ATP as a Δ*spxB* or *spxB*$^+$ strain. Acetate addition and anaerobic growth experiments suggested decreased ATP, rather than increased AcP, as a reason that Δ*ackA* mutants accumulated *spxB* or *spxR* suppressors, although experimental manipulation of the AcP amount was limited. This finding and other considerations suggest that coping with endogenously produced H_2O_2 may require energy. Starting with a Δ*spxB* mutant, we constructed Δ*pta*, Δ*ackA*, and Δ*pta* Δ*ackA* mutants. Epistasis and microarray experiment results were consistent with a role for the SpxB-Pta-AckA pathway in expression of the regulons controlled by the WalRK$_{Spn}$, CiaRH$_{Spn}$, and LiaSR$_{Spn}$ TCSs involved in sensing cell wall status. However, AcP likely does not play a physiological role in TCS sensing in *S. pneumoniae*.

Streptococcus pneumoniae (pneumococcus) is a major human respiratory pathogen that causes over 1.6 million deaths worldwide annually (19, 23, 51). *S. pneumoniae* is a Gram-positive, ovococcal-shaped bacterium that is usually found as a diplococcus or as short chains of cells (3, 58). *S. pneumoniae* colonizes, often asymptomatically, the nasopharynx of 10 to 20% of healthy adults and 40 to 60% of young children (51). Colonization is the major reservoir for transmission of *S. pneumoniae* among humans, its major host (9, 23, 51). Colonization can also progress to serious invasive diseases, including pneumonia, otitis media (earache), meningitis, and bacteremia in susceptible individuals (7, 29, 30, 51). During colonization and invasive disease, pneumococcus encounters diverse environments and changes in temperature and availability of oxygen, metal ions, and nutrients (2, 5, 17, 18, 21, 24, 39, 47). Pneumococcus must also contend with innate and humoral immune responses (23, 51). Many genes involved in bacterial adaptation, survival, and virulence encode enzymes that mediate central metabolism and maximize energy production (44). These links are only starting to be studied systematically in *S. pneumoniae*, and they provide promise in identifying targets for antibiotic development to combat emerging multidrug resistance (12, 29).

* Corresponding author. Mailing address: Department of Biology, Indiana University Bloomington, Jordan Hall 142, Bloomington, IN 47405. Phone: (812) 856-1318. Fax: (812) 855-6705. E-mail: mwinkler@bio.indiana.edu.

† Supplemental material for this article may be found at http://jb.asm.org/.

▽ Published ahead of print on 15 October 2010.

S. pneumoniae is an aerotolerant anaerobe with fermentative metabolism. It lacks a tricarboxylic acid (TCA) cycle and an electron transport chain, and its central metabolism consists primarily of glycolysis (Fig. 1) (20, 28, 48). Pneumococcus catabolizes glucose and other sugars by glycolysis to generate two molecules of ATP by substrate-level phosphorylation and produce pyruvate, which is converted to acetyl coenzyme A (CoA) and other metabolites, including acetyl phosphate (AcP) (Fig. 1) (14). AcP can be converted by acetate kinase (AckA) to ATP and acetate to generate an additional molecule of ATP (53, 54). Under aerobic conditions with glucose as the primary carbon source, pneumococcus produces mainly lactate and a small amount of acetate as fermentation products, whereas a mixture of acids and ethanol are produced from other sugars, such as galactose (56).

Three metabolic enzymes lead to the synthesis of AcP in *S. pneumoniae* (Fig. 1). SpxB pyruvate oxidase uses molecular oxygen and inorganic phosphate to convert pyruvate directly into AcP and H_2O_2 (40, 42, 45, 47). SpxB is present in only a limited number of bacterial species (26, 42) and is the major source of the significant amount (≈1 mM) of endogenous H_2O_2 secreted in *S. pneumoniae* cultures (40, 42, 45, 47). Previously, we demonstrated that *spxB* transcription is positively regulated by the novel CBS-HotDog domain protein SpxR, which may link the SpxB amount to energy and metabolic state (42). Cellular AcP amounts are reduced by 80% in exponentially growing Δ*spxB* mutants, and it was inferred, but not shown directly, that cellular ATP amount may also be decreased (40). Despite this large drop in cellular AcP amount (40) and a decrease in H_2O_2 production of 90% (42), we

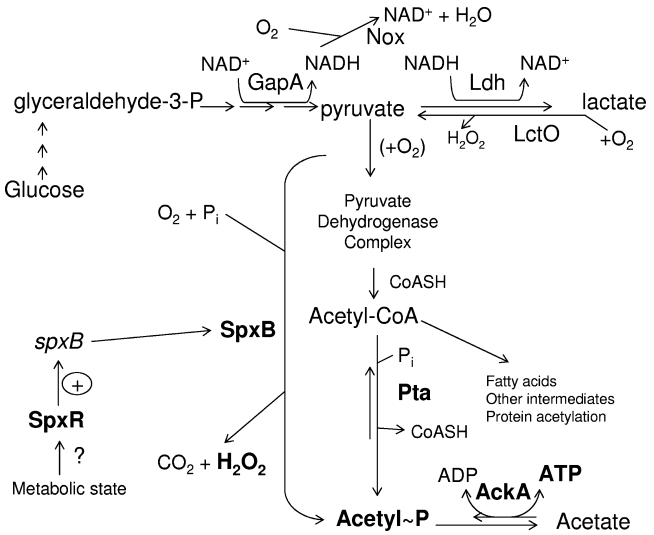

FIG. 1. Model of central metabolism in *S. pneumoniae* growing aerobically in glucose-containing BHI broth. An abbreviated version of the Embden-Meyerhof-Parnas glycolytic pathway is shown; this pathway converts glucose to pyruvate and generates two ATP molecules. Pyruvate is converted to lactate by lactate dehydrogenase (Ldh), regenerating NAD^+, and lactate can be converted back to pyruvate by lactate oxidase (LctO). NADH oxidase (Nox) also converts NADH back to NAD^+. Pyruvate is converted to acetyl-CoA by the pyruvate dehydrogenase complex. Acetyl~P (AcP) is formed from acetyl-CoA by Pta or from pyruvate by pyruvate oxidase (SpxB), which also produces H_2O_2. Transcription of the *spxB* gene is positively regulated by the SpxR CBS-HotDog domain regulator. Acetyl~P is converted to acetate and another molecule of ATP by AckA. See the text for additional information and references.

detected only limited changes in global transcription patterns in a Δ*spxB* mutant compared to its *spxB*$^+$ parent (42). This result suggested that AcP does not play a major role in pneumococcal signaling, although we could not rule out that the total cellular AcP amount remained large enough in Δ*spxB* mutants to mask changes in signaling or that compensatory metabolic pathways operate in Δ*spxB* mutants. Curiously, Δ*spxB* mutants treated with high (20 mM) concentrations of exogenously added H_2O_2 seem to have greatly reduced ATP pools and die rapidly (40, 42).

The two other pneumococcal enzymes that synthesize AcP comprise the phosphotransacetylase (Pta)-AckA pathway, which is widely distributed in other bacteria (Fig. 1) (11, 53, 54). There has been controversy about whether *S. pneumoniae* possesses an active pyruvate dehydrogenase under aerobic growth conditions (56). In work to be presented elsewhere, we demonstrate the presence of a functional pyruvate dehydrogenase (unpublished data). Acetyl-CoA produced by this complex is converted by Pta to AcP (Fig. 1) (reviewed in reference 53). AckA converts AcP produced by Pta or SpxB to acetate and ATP, or in the reverse direction, acetate to ADP and AcP (Fig. 1). In bacteria lacking electron transport and a TCA cycle, such as *S. pneumoniae*, AckA is thought to play an important role in providing additional ATP from pyruvate (53, 54). The Pta-AckA pathway has been studied extensively in *Escherichia coli* and *Salmonella* species (reviewed in references 53 and 54). In these and other bacteria, response regulators from several two-component regulatory systems (TCSs) are phosphorylated by AcP *in vitro* and *in vivo*, and it has been suggested that AcP phosphorylation links regulation of these TCSs to metabolic state (13, 15, 25, 54). In addition, acetyl-CoA from the Pta-AckA pathway serves as an acetyl group donor to numerous proteins, including RNA polymerase, thereby modulating their activities and functions (53, 54). Despite its likely importance to metabolism and signaling, the Pta-AckA pathway has not been characterized in *S. pneumoniae.* Moreover, precedents from other bacteria like *E. coli* and *Salmonella* species cannot be applied to pneumococcus, because those organisms possess a different central metabolism and lack the SpxB pyruvate oxidase that produces AcP.

This study provides the first characterization of the contribution of the Pta-AckA pathway to pneumococcal metabolism, specifically, ATP and AcP production, and its links to the reaction catalyzed by SpxB. By constructing strains containing combinations of mutations resulting in a defective SpxB-Pta-AckA pathway, we show that cellular ATP amounts are affected by abolishment of AcP production and lack of AckA function. Surprisingly, we found that Δ*ackA* mutants are unstable and rapidly accumulate suppressor mutations that inactivate SpxB or SpxR. The basis for this suppression and the possible role of AcP in TCS signaling were tested by a combination of epistasis analysis, microarrays, and determinations of ATP and AcP amounts. The results were consistent with an energy-dependent process that protects *S. pneumoniae* from endogenously produced H_2O_2 and a role for the SpxB-Pta-AckA pathway in expression of regulons controlled by a specific subset of TCSs, although a physiological role for AcP in pneumococcal response regulator phosphorylation seems unlikely.

MATERIALS AND METHODS

Bacterial strains and growth conditions. Bacterial strains used in this study are listed in Table S1 of the supplemental material. All cultures were grown statically with limited aeration in brain heart infusion broth (BHI; Becton-Dickinson [BD]) or on blood agar (BA) plates containing Trypticase soy agar II modified (BD) and 5% (vol/vol) defibrinated sheep blood (Remel) at 37°C in an atmosphere of 5% CO_2. Growth was monitored directly by measuring the optical density at 620 nm (OD_{620}) using a Spectronic 20 Genesys spectrophotometer. Overnight cultures of strains were started by inoculating frozen bacterial stocks into 17-mm-diameter polystyrene plastic tubes containing 5 ml of BHI broth and then performing 100-fold serial dilutions over five tubes. Overnight cultures were incubated between 15 and 18 h, and cultures with an OD_{620} of 0.1 to 0.4 were used to inoculate final BHI broth cultures lacking antibiotics to an OD_{620} of 0.005.

Construction and verification of mutant strains. The mutant strains (listed in Table S1 of the supplemental material) were constructed by transformation of competent *S. pneumoniae* cells with linear PCR amplicons as described previously (37, 43). Briefly, antibiotic resistance markers were introduced into amplicons by overlapping PCR using the primers listed in Table S2 of the supplemental material. *S. pneumoniae* cells were induced to competence by the addition of synthetic competence stimulatory peptide. Transformants were selected on BA plates containing antibiotics at the concentrations listed in Table S1. Markerless deletions and point mutations were constructed using the two-step Janus method of allelic replacement in a *rpsL1* (streptomycin-resistant) genetic background (42, 46). In the first step, the Kan^r-*rpsL*$^+$ Janus cassette was crossed into genes of interest from PCR amplicons by selection for kanamycin resistance and screening for streptomycin sensitivity. In the second step, the Janus cassette was replaced by transformation with a PCR amplicon containing the desired mutations by selection for streptomycin resistance and screening for kanamycin sensitivity. Final transformants were isolated as single colonies three times on BA plates containing antibiotics and propagated for storage in BHI broth containing antibiotics as needed. All constructs were confirmed by PCR amplification and sequencing as described previously (42).

Quellung reaction. To determine the presence or absence of capsule, the Quellung reaction was performed on colonies from BA plates or on BHI broth cultures (28). Briefly, an overnight colony was transferred from a plate to a glass microscope slide and mixed with 1.5 μl of 1× phosphate-buffered saline (PBS; Ambion), or 1.5 μl of a broth culture at an OD_{620} of 0.05 was transferred onto a microscope slide. A 1.5-μl volume of type 2 capsule serum (Statens Serum Institute) was added and mixed with the sample. A glass coverslip was placed on the sample, and the slide was observed on a Nikon E-400 phase-contrast microscope with a 100× oil immersion objective. If capsule was present, the cell surface appeared to swell after addition of the serum, whereas if capsule was absent, there was no change in the appearance of the cells.

Hydrogen peroxide release assay. The rate of H_2O_2 production was determined using the Amplex Red hydrogen peroxide/peroxidase assay kit (Invitrogen) as previously described (42).

Biofilm characterization. Biofilms on the sides and bottoms of tubes containing overnight bacterial cultures were visualized and quantitated with crystal violet. Overnight BHI broth cultures in 17-mm-diameter polystyrene plastic tubes were grown as described above. Culture supernatants of unattached cells that had reached an OD_{620} of 0.5 to 0.6 were removed from overnight tubes, and biofilms were gently washed twice with 500 μl of room temperature PBS. A 500-μl mixture of 0.15% (wt/vol) crystal violet, 8.2% (vol/vol) ethanol, 0.4% (vol/vol) methanol was added and incubated at room temperature for 20 min. The staining solution was removed, and biofilms were rinsed four times with 1 ml of PBS. Retained crystal violet stain was dissolved with 2 ml of 95% (vol/vol) ethanol for 20 min, and a sample was diluted 10-fold in 95% (vol/vol) ethanol. The A_{550} of the dissolved crystal violet was determined in 96-well plates by using a microplate reader (Molecular Dynamics) and normalized to the OD_{620} of the culture supernatants.

ATP and AcP determinations. ATP and AcP amounts were assayed using the Cell Titer Glo reagent (Promega) as described previously (40, 41) with the following modifications. Twenty-milliliter cultures of desired strains were grown in 50-ml polystyrene tubes to early exponential phase (OD_{620}, 0.2). In contrast to the protocol described in reference 40, cells were not heated during ATP extraction, and the same initial extraction procedure was used for ATP and AcP determinations. Cells were collected by centrifugation for 5 min at 10,000 × *g* at 4°C and washed twice with 250 μl of cold buffer A (10 mM sodium phosphate [pH 7.5], 10 mM $MgCl_2$, and 1 mM EDTA). Aliquots (50 μl) of cell suspension were set aside on ice for protein assays. A 50-μl volume of cold 3.0 M $HClO_4$ was added to the remaining 200 μl of cell suspension and incubated on ice for 30 min. After incubation, tubes were centrifuged for 2 min at 8,000 × *g* at 4°C. The supernatant was transferred to an empty tube, neutralized by the addition of 75 μl of saturated $KHCO_3$ (36 g $KHCO_3$ in 100 ml H_2O), and centrifuged at 8,000 × *g* at 4°C.

For ATP determinations, duplicate 50-μl samples of supernatant were each mixed with 50 μl of Cell Titer Glo reagent (reconstituted according to the manufacturer's instructions) in wells of a white, opaque 96-well flat-bottom plate (Falcon). Plates were incubated for 10 min at room temperature, and luminescence was measured using a Spectra Max fluorescence plate reader running Soft Max Pro software (Molecular Devices). ATP concentrations were determined by comparison with standard curves of known concentrations of ATP (0.5 to 10.0 μM) freshly diluted in buffer A to which acid and base had been added as described above. All sample concentrations fell within the ranges of standard curves (data not shown).

For AcP assays, $KHCO_3$-neutalized supernatants were transferred to empty tubes, and 15.0 mg of powdered activated charcoal (Sigma) was added to bind ADP and ATP in the extracts. Tubes were vortexed and incubated on ice for 15 min. Charcoal was removed by filtration through a 13-mm-diameter syringe filter (0.22-μm pore size), and extracts were collected into new tubes. Fifty-microliter samples were assayed as described above as a control for ATP removal by the charcoal treatment. Remaining AcP in samples was enzymatically converted to ATP. Samples of 100 μl were mixed with 1.0 μl of 100 mM $MgCl_2$, 30 μl of 100 μM ADP, and 1.0 μl of 0.4-μg/μl purified *E. coli* acetate kinase (Sigma) (final concentrations of 1 mM $MgCl_2$, 30 μM ADP, and 4 μg acetate kinase per ml). Reaction mixtures were incubated at 30°C for 90 min. After incubation, duplicate 50-μl aliquots were each mixed with 50 μl of Cell Titer Glo reagent, and ATP amounts were determined as described above, except the buffer for the standards was treated with activated charcoal and filtered like the test samples before known amounts of ATP were added.

All measurements were normalized to protein amounts in the extracts. Fifty-microliter samples that were set aside for protein assays were centrifuged at 16,000 × *g* at 4°C for 2 min. Cell pellets were suspended in 200 μl of 1% (wt/vol) SDS and 0.1% (vol/vol) Triton X-100 and mixed vigorously by vortexing. Protein amounts were determined in duplicate 5-μl samples using the DC protein assay kit (Bio-Rad) according to the manufacturer's instructions.

To validate these assays, a series of control experiments was performed. The first control ensured that AcP was fully recovered within the experimental error range in the extraction and that conversion of AcP to ATP was driven to completion. This control was done by adding a range of known amounts of AcP at the beginning of the extraction procedure and assaying the conversion of added AcP to ATP. The second control confirmed that the ATP produced in the AcP assay was obtained from the enzymatic reaction. Two separate reactions, one lacking purified AckA and one in which the extract was heated to 100°C for 5 min, were assayed and found to lack ATP production. In the third control experiment, we assayed ATP amounts in *S. pneumoniae* and *E. coli* cultures in side-by-side comparisons using two different extraction procedures that had been published previously for *E. coli* (6, 25). Similar results were obtained for *S. pneumoniae* when using either procedure, and we obtained results comparable to those published previously for *E. coli* (6, 25, 36).

Cellular content and concentrations of ATP and AcP (see Table 2 below) were estimated using the following parameters: (i) 0.42 ± 0.02 mg of protein (mean ± standard error; $n = 8$) was recovered from 20 ml of strain IU1781 at an OD_{620} (1-cm path length) of 0.2 by the procedure described above. A comparable amount of protein was recovered from unencapsulated strain IU1945. (ii) An OD_{620} (1-cm path length) of 0.2 corresponded to 5.5×10^7 CFU per ml for strain IU1781. A similar CFU per ml was obtained for strain IU1945. (iii) Strain IU1781 chains (≈11 cells per chain in BHI broth [3]) were disrupted to mostly diplococci by the vigorous mixing during serial dilution in PBS and brief heating in nutrient broth-soft agar used in the determinations of CFU per ml. Therefore, each CFU of strain IU1781 corresponded to a diplococcus of two cells, as with strain IU1945 (3). Disruption of strain IU1781 chains accounted for the observations that the CFU per ml per OD_{620} unit and protein yield (cell mass) per OD_{620} unit were similar for strains IU1781 and IU1945. (iv) The volume of strain IU1781 cells, $\approx 0.6 \times 10^{-15}$ liter, was based on the cell dimensions described in reference 3. Consistent with these assumptions, the ATP content per mg of protein and ATP concentrations were similar for strains IU1781 and IU1945 (data not shown). Based on these considerations, the amount of protein recovered by this method was ≈200 μg per 1×10^9 pneumococcal cells.

RNA extraction and microarray analysis. Final cultures were started at an OD_{620} of ≈0.001 in BHI broth and grown to early exponential phase (OD_{620}, ≈0.1). Rapid lysis RNA extraction, purification, cDNA synthesis, labeling, hybridization to *S. pneumoniae* R6 microarrays (Ocimum Biosolutions), array washing, and data collection were performed as described previously (24, 28). Data were collected from one to four independent biological replicates, including dye swaps, and analyzed using software from the TM4 microarray software suite (www.tm4.org). Result files generated by GenePix Pro 6.0 software (Molecular Devices) were converted to the TIGR MultiExperiment Viewer file format using the ExpressConverter 2.1 software. Lowess (block) data normalization was performed using the TIGR MIDAS 2.21 software. Expression ratios and Bayesian *P* values were calculated as described previously (24, 28). The cutoff for significant changes in relative transcript amounts was set at ±1.8-fold, with a Bayesian *P* value of <0.001, when available.

Microarray data accession number. Microarray data (intensity and expression ratio) were deposited in the GEO database (www.ncbi.nlm.nih.gov/geo/) under accession number GSE23404.

RESULTS

Deletion of *ackA* leads to accumulation of suppressor mutations. The *S. pneumoniae* serovar 2 D39 genome contains a single *ackA* ortholog (*spd_1853*) (28), whose gene product matches the amino acid sequence of *E. coli* acetate kinase ($AckA_{Eco}$) over its whole length (data not shown). $ackA_{Spn}$ is preceded by a gene encoding an adenine-specific DNA methylase, characteristic of a restriction system methylase. A DNA methylase gene precedes *ackA* in several low-GC Gram-positive species (31). $ackA_{Spn}$ is followed by a strong predicted transcription terminator in a 151-bp intercistronic region that precedes essential *rnpA* (encoding the protein subunit of RNase P). A linear amplicon containing a Δ*ackA*::Kan^r *rpsL*$^+$ deletion/insertion mutation was synthesized that removed all but the first and last 60 bp of the *ackA* gene (see Materials and

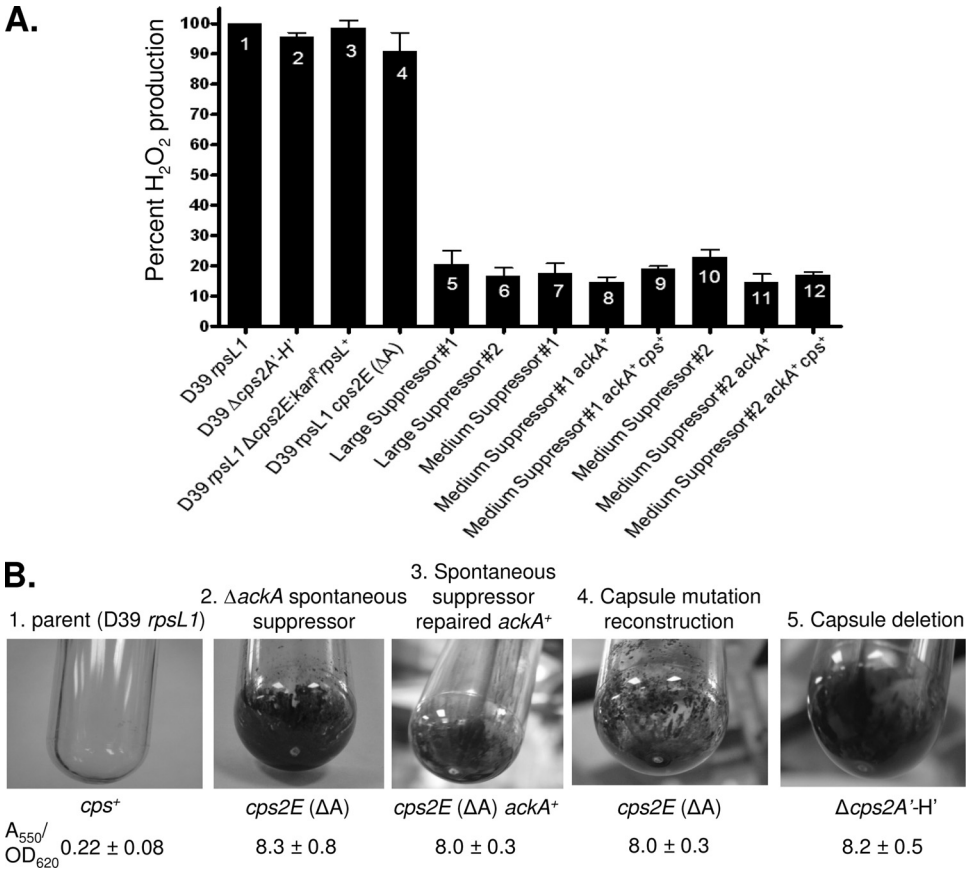

FIG. 2. H_2O_2 production (A) and biofilm formation (B) by Δ*ackA* suppressor mutants. (A) H_2O_2 production was determined relative to the parent strain (IU1781; bar 1) in limited aeration (static) cultures as described in Materials and Methods, and standard errors from multiple independent determinations are indicated. Bars 2 to 4, constructed unencapsulated mutants; bars 5 and 6, mucoid large colony suppressors; bars 7 and 10, medium-size rough colony suppressors; bars 8, 9, 11, and 12, medium-sized rough colony suppressors in which the Δ*ackA* and *cps2E* (ΔA) mutations were repaired to the *ackA*$^+$ and *cps2E*$^+$ alleles. Relevant genotypes are shown and are also listed in Table S1 of the supplemental material. Bar 2, strain IU1945; bar 3, IU3286; bar 4, IU3309; bar 5, IU3254; bar 6, IU3255; bar 7, IU3250; bar 8, IU3252; bar 9, IU3311; bar 10, IU3251; bar 11, IU3253; bar 12, IU3313. (B) Biofilms formed by overnight cultures in polystyrene tubes were stained with crystal violet and quantitated based on the A_{550} as described in Materials and Methods. Panels from left: 1, parent encapsulated strain IU1781; 2, unencapsulated strain IU3250, a rough, medium-sized colony Δ*ackA* suppressor containing the *spxB* (Trp339STOP) and *cps2E* (ΔA) mutations; 3, unencapsulated strain IU3252, medium-sized rough colony suppressor IU3250 repaired back to *ackA*$^+$; 4, unencapsulated strain IU3309, an *ackA*$^+$ *spxB*$^+$ strain containing the constructed *cps2E* (ΔA) allele; 5, unencapsulated strain IU1945, an *ackA*$^+$ *spxB*$^+$ strain containing the large Δ*cps2A′*-Δ*cps2H′* deletion. See Table S1 for full genotypes. A_{550} values after crystal violet staining were normalized to the density (OD_{620}, ≈0.5 to 0.6) of the culture supernatants containing unattached cells. Averages are based on three or more independent determinations, and standard errors are indicated.

Methods; see also Tables S1 and S2 in the supplemental material). Transformation of this Δ*ackA* amplicon into the D39 *rpsL1* parent strain led to the appearance of three types of colonies: very small, smooth colonies; medium-size, rough colonies of about the same size as the parent; and larger mucoid colonies. This size variation suggested the accumulation of spontaneous suppressor mutations.

Consistent with this interpretation, restreaking the very small Δ*ackA* colonies on BA plates led to the appearance of all three colony types. In contrast, the medium and large colonies were stable during restreaking and were characterized further (described below). Expression of a copy of the *ackA*$^+$ gene from a fucose-inducible promoter (P_{fcsK}) in the ectopic CEP site (IU4352 [see Table S1]) (50) complemented the instability of the Δ*ackA* mutant on BA plates. In this background, transformants containing the Δ*ackA* mutation formed normal-looking colonies when 0.2% (wt/vol) fucose was added to plates but formed the three sizes of colonies described above when fucose was omitted (data not shown). Finally, it should be noted that the *rpsL1* allele was included in these strains to allow markerless mutant construction by allele exchange (see Materials and Methods; see also Tables S1 and S2 in the supplemental material) (42, 46). In many constructs, *rpsL1* was complemented directly by the presence of the Kan^r *rpsL*$^+$ cassette. In other strains, the *rpsL1* allele did not affect the phenotypes reported here (data not shown).

Biofilm formation by the medium-size colonies was caused by mutations in the capsule locus. The Δ*ackA* mutants that formed medium-size rough colonies had two distinct phenotypes. They produced only ≈10% H_2O_2 compared to the parent strain (Fig. 2A, bars 7 and 10), and they formed biofilms in BHI broth cultures in polystyrene tubes, as visualized by crystal violet staining (Fig. 2B, tube 2). Repair of the Δ*ackA* deletion back to the wild-type *ackA*$^+$ allele did not decrease biofilm

formation (Fig. 2B, tube 3), indicating that the biofilm formation phenotype was caused by accumulation of another mutation in this class of Δ*ackA* mutant. In *S. pneumoniae*, there is an inverse relationship between biofilm formation and capsule production in culture (reviewed in reference 33). Encapsulated strains, such as the parent D39 *rpsL1* strain (Fig. 2B, tube 1), do not form robust biofilms in culture, whereas unencapsulated mutants form biofilms (Fig. 2B, tube 5) (1, 33, 35). The Quellung antibody test for serotype 2 capsule confirmed that the medium-size Δ*ackA* mutants were indeed unencapsulated (data not shown). In contrast, the very small unstable Δ*ackA* mutants and large mucoid suppressors produced capsule.

The capsule biosynthesis locus in *S. pneumoniae* D39 contains 17 genes (reviewed in reference 57). Previous studies showed that mutations that limit or prevent capsule biosynthesis only occur in the first five genes, *cps2ABCDE*, which are involved in initiating sugar repeat unit formation and regulating capsule chain length and amount (55, 57). Mutations in the other *cps2* genes eliminate side chain assembly, transport, and polymerization and are lethal to cells, unless suppressed by mutations that inactivate *cps2E* (55), which encodes the initiating repeat unit glycosyltransferase (8). An insertion in *cps2E* also turned up in a transposon screen of genes that affect pneumococcal biofilm formation (35). For these reasons, we amplified and sequenced the 3.7-kb region containing *cps2CDET′* from nine independently isolated Δ*ackA* medium-size colony suppressors (Table 1). These strains contained mutations in *csp2E* (7/9) or *cps2C* (2/9), five of which were frameshift mutations. One mutation, *cps2E* (ΔA), consisting of a deletion of 1 A from a run of 7 A bases, arose three times independently and was used in subsequent experiments.

Spontaneous mutations leading to loss of capsule were not associated with reduced H_2O_2 production in Δ*ackA* mutants. Medium-size Δ*ackA* mutants containing the *cps2E* (ΔA) mutation produced low levels of H_2O_2 (Fig. 2A, bars 7 and 10). To determine if this phenotype was caused by the combination of Δ*ackA* and *cps2E* (ΔA) mutations, we repaired the Δ*ackA* allele alone and then both the Δ*ackA* and *cps2E* (ΔA) mutations back to their wild-type alleles and assayed H_2O_2 production (Fig. 2A, bars 8, 9, 11, and 12). We also constructed and assayed isogenic strains containing a Δ*cps2E* deletion/insertion or the *cps2E* (ΔA) mutation (Fig. 2A, bars 3 and 4, and B, tube 4). H_2O_2 production was comparable in the *cps2E* mutants and the *cps2E*$^+$ parent (Fig. 2A, bar 1), whereas all strains in which the Δ*ackA* or *cps2E* (ΔA) alleles were repaired still produced relatively low levels of H_2O_2 (Fig. 2A, bars 7 to 12), indicating that the medium-size Δ*ackA* mutants contained a second suppressor mutation that decreased H_2O_2 production.

Mutations in *spxB* and *spxR* suppress the deleterious effects of Δ*ackA* deletion. The Δ*ackA* mutants that formed larger, mucoid colonies retained capsule and showed a decrease in H_2O_2 production similar to that of the medium-size, rough Δ*ackA* mutants (Fig. 2A, bars 5, 6, and 10). Since both medium- and large-size Δ*ackA* colonies were defective in H_2O_2 production (Fig. 2A), we sequenced the *spxB* and *spxR* genes (Fig. 1) (42) of seven independent Δ*ackA* suppressor strains (Table 1). Five isolates had spontaneous lesions in the *spxB* reading frame, including one frameshift and one nonsense mutation, one isolate had a change in the mapped transcription start site of *spxB* from G to T, and one had a frameshift mutation in *spxR*. All of the mutations were different and likely reduced SpxB activity or expression as reflected by reduced H_2O_2 production (data not shown).

TABLE 1. Spontaneous suppressor mutations that accumulated in Δ*ackA* mutants

Phenotype group and mutated gene	Mutation in independent isolates
Mucoid large colony suppressors	
spxB	Phe269Leu (TTT to CTT)
spxB	Frameshift mutation ΔC in codon 264
spxB	Gly472Asp (GGC to GAC)
spxB	Change in mapped transcription start from G to T
Rough medium-sized colony suppressors	
spxB	Trp339STOP (TGG to TAG)
cps2E[a]	Frameshift mutation ΔA in codon 326 (in run of 7 As)
spxB	Gly423Cys (GGT to TGT)
cps2E[a]	Frameshift mutation ΔA in codon 326 (in run of 7 As)
spxR	Frameshift mutation ΔG in codon 115 (in run of 5 Gs)
cps2E[a]	Frameshift mutation ΔA in codon 326 (in run of 7 As)
Additional capsule mutations identified in rough medium-sized colony suppressors	
cps2E	Frameshift mutation ΔG in codon 111
cps2E	Arg347Cys (CGT to TGT)
cps2E	Frameshift mutation ΔA in codon 419
cps2E	Insertion of T after codon 204
cps2C	Insertion of A after codon 45
cps2C	Insertion of T in codon 113

[a] Isolated three times from separate independent transformations.

These results suggested that inactivation of *spxB* or *spxR* stabilized Δ*ackA* deletion strains. This conclusion was corroborated in two ways. First, transformation of the Δ*ackA* deletion into Δ*spxB* or *spxR*::Mariner null mutants (IU2173 or IU2072, respectively [see Table S1 in the supplemental material]) resulted in uniform, large, mucoid colonies, similar to the appearance of one class of the spontaneous suppressors (data not shown). Second, Δ*ackA* transformants with uniform colony size and morphology were obtained in the D39 *rpsL1* parent strain under anaerobic conditions, in which SpxB is not functional (Fig. 1). When Δ*ackA* transformants obtained under anaerobic conditions were streaked onto aerobic plates, the same mixture of colony sizes described above was observed. We also confirmed that a constructed *cps2E* (ΔA) mutation alone did not stabilize Δ*ackA* mutants (data not shown). Finally, various strain constructions confirmed that *spxB cps2* or *spxB* mutants alone formed medium-sized rough or large mucoid colony morphologies, respectively, similar to those observed for the spontaneous Δ*ackA* suppressor mutants. Together, these findings suggested that the medium-sized rough colonies resulted

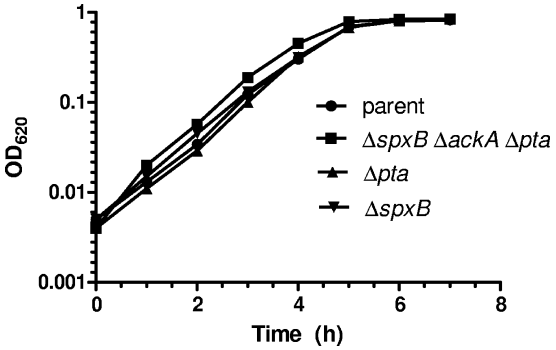

FIG. 3. Typical growth curves of encapsulated parent strain IU1781 (D39 *rpsL1*) and isogenic mutants IU2837 (D39 *rpsL1* Δ*spxB* Δ*pta* Δ*ackA*), IU2687 (D39 *rpsL1* Δ*pta*), and IU2173 (D39 *rpsL1* Δ*spxB*) in BHI broth at 37°C with limited aeration (static) in an atmosphere of 5% CO_2 (see Materials and Methods). See Table S1 of the supplemental material for full genotypes. The experiment was repeated numerous times.

from tandem mutation, starting with inactivation of capsule biosynthesis followed by inactivation of *spxB* or *spxR*.

Δ*pta* deletion is not deleterious to cells. In contrast to Δ*ackA* mutants, deletion of *pta* did not cause overt accumulation of spontaneous suppressor mutations. The *S. pneumoniae* serovar 2 D39 genome contains only a single ortholog of *pta* (*spd_0985*) (28). Similar to Pta from other low-GC Gram-positive bacteria, Pta_{Spn} lacks the extra amino-terminal domains present in Pta from *E. coli* and related species (data not shown). pta_{Spn} is preceded by *rluD* (putative pseudouridine synthase) and followed by a 270-bp intercistronic region preceding an oppositely oriented IS*1167* element (data not shown). Because of PCR amplification issues, the Δ*pta*::Kan^r *rpsL*$^+$ insertion/deletion mutation retained only the last 200 bp of *pta* (see Tables S1 and S2 in the supplemental material). The only phenotypic change for Δ*pta* mutants was formation of slightly smaller colonies than the parent strain on BA plates incubated in an atmosphere of 5% CO_2 (data not shown). This slight growth defect was complemented by expression of *pta*$^+$ under the control of a fucose-inducible promoter from the ectopic CEP site (strain IU4497 [see Table S1]) (data not shown). However, there was no defect in relative growth rate or yield of the Δ*pta* mutant grown in BHI broth under similar incubation conditions (Fig. 3). The Δ*pta* mutant formed normal-sized colonies on anaerobic BA plates, and Δ*pta* Δ*spxB* mutants formed large, mucoid colonies indistinguishable from Δ*spxB* mutants on plates incubated aerobically. These observations suggest that Δ*pta* mutants may be slightly inhibited by aerobic growth on plates but not in certain complex broths grown with limited aeration. Consistent with its similar growth in BHI broth, relative transcript amounts of the exponentially growing Δ*pta* mutant showed relatively few differences compared to its isogenic *pta*$^+$ parent (see Table S3 in the supplemental material). Notably, there were moderate increases in the relative transcript amounts of the *prtA* gene (cell wall-associated serine protease) and *psa* regulon (manganese transport), but little else, in the Δ*pta* mutant compared to its parent. Finally, unlike deletion of *spxB*, deletion of *pta* did not stabilize a Δ*ackA* mutant, and the three sizes of colonies described above appeared for the Δ*pta* Δ*ackA* mutants (data not shown). Together, these results indicated that we could construct mutants containing single Δ*spxB* or Δ*pta* mutations, both Δ*spxB* and Δ*pta* mutations, or combinations of Δ*ackA*, Δ*spxB*, and Δ*pta* mutations, provided that Δ*spxB* mutations were introduced before Δ*ackA* mutations to stabilize strains (see Table S1 in the supplemental material).

Characterization of cellular ATP and AcP amounts in Δ*ackA*, Δ*spxB*, and Δ*pta* mutant combinations. Δ*ackA* mutants are blocked in the conversion of AcP to acetate and ATP (Fig. 1) (53). Therefore, the immediate effect of blocking the AckA step would be a decrease in the cellular ATP amount and a possible accumulation of AcP. In contrast, decreased activity or expression of SpxB decreases AcP amount (40) and H_2O_2 production. To better understand the effects of these mutations on the SpxB-Pta-AckA pathway (Fig. 1), we determined the relative amounts of ATP and AcP in these mutants and their parent strain growing exponentially in BHI broth (see Materials and Methods). All samples were taken in early exponential phase, when the bacteria are primarily excreting lactate and little acetate and before significant depletion of the glucose contained in BHI broth (47).

In contrast to a preliminary result suggesting much greater amounts of AcP than ATP (40), we found that the amount of AcP was only ≈1.5-fold greater than that of ATP in *S. pneumoniae* D39 (Table 2). We estimated that the cellular concentrations of extractable ATP and AcP were ≈2 mM and ≈3 mM, respectively, under these culture conditions (Table 2; row 1). Validation experiments in which *E. coli* cells were extracted in parallel experiments gave cellular ATP concentrations of ≈3.0 mM, which is comparable to values reported previously (6, 25, 36). Different extraction formats which increased the yield of ATP from *E. coli* (6) did not appreciably affect the yield of ATP from *S. pneumoniae* (data not shown). We conclude that the ATP pool in *S. pneumoniae* is comparable to that of *E. coli* during exponential growth in rich media.

We noted strong homeostasis to maintain cellular ATP amounts in *S. pneumoniae* by the parallel SpxB and Pta routes (Fig. 1). Addition of 15 mM potassium acetate to the medium increased the relative cellular amount of AcP by ≈1.6-fold, which was the maximum that could be obtained by acetate addition, but the relative amount of ATP remained unchanged (Table 2, row 2). Δ*spxB* mutants contained only about 20% of the AcP of the parent strain, but again ATP amount was maintained. This finding supports the previous report that the relative amount of AcP is reduced to 20% in *spxB* mutants (40). Δ*pta* mutants had the same amounts of ATP and AcP as the parent strain (Table 2, row 4), and addition of 15 mM potassium acetate to the Δ*pta* mutant increased the relative AcP amount by ≈1.5-fold but left the relative ATP amount unchanged (Table 2, row 5).

In contrast, Δ*spxB* Δ*ackA* mutants contained only about half the ATP amount of the parent strain and accumulated about twice as much AcP in the dead-end pathway created by the absence of SpxB and AckA (Fig. 1; Table 2, row 6). Consistent with this result, the Δ*spxB* Δ*pta ackA*$^+$ mutant showed the same 50% reduction in relative ATP amount and contained negligible AcP, indicating little conversion of acetate to AcP by AckA under the growth conditions sampled here. The Δ*spxB* Δ*pta* Δ*ackA* triple mutant could be readily constructed starting with the Δ*spxB* mutation to suppress the Δ*ackA* mutation (see

TABLE 2. Relative cellular amounts of ATP and AcP in the parent D39 strain and SpxB-Pta-AckA pathway mutants growing exponentially in BHI broth

Strain[a]	Presence of gene			Addition[b]	Relative amt (*n*)[c]	
	spxB	*pta*	*ackA*		ATP[d]	AcP[e]
IU1781	+	+	+	None	≡1 (9)	≡1 (8)
IU1781	+	+	+	15 mM potassium acetate	1.0 ± 0.05 (3)	1.6 ± 0.10 (2)
IU2173	−	+	+	None	1.0 ± 0.08 (3)	0.18 ± 0.02 (3)
IU2687	+	−	+	None	1.1 ± 0.06 (3)	1.0 ± 0.10 (3)
IU2687	+	−	+	15 mM potassium acetate	0.90 ± 0.08 (2)	1.5 ± 0.10 (2)
IU3590	−	+	−	None	0.53 ± 0.04 (3)	1.9 ± 0.20 (2)
IU2689	−	−	+	None	0.50 ± 0.05 (3)	0.08 ± 0.04 (3)
IU2837	−	−	−	None	0.54 ± 0.09 (3)	0.07 ± 0.01 (3)

[a] Further information on the indicated strains is provided in Table S1 of the supplemental material. The presence of capsule was confirmed by smooth colony formation on BA plates and Quellung reactions (see Materials and Methods).

[b] Potassium acetate (CH_3CO_2K) was added to some cultures at a final concentration of 15 mM at the beginning of culture growth.

[c] Bacteria were grown to an OD_{620} of 0.2, and relative cellular amounts of ATP and AcP were determined as described in Materials and Methods. The number of biological replicates (*n*) is indicated, and determinations were performed in duplicate within each replicate experiment.

[d] The amount of ATP recovered from 20 ml of encapsulated strain IU1781 (D39 *cps*$^+$ *rpsL1*) cells at an OD_{620} of 0.2 was 0.0067 μmol/mg of protein extract. This amount corresponds to an estimated cellular concentration of ≈2 mM ATP (see Materials and Methods). The experimental error of the ATP determinations was ≈8%.

[e] The amount of AcP recovered from 20 ml of IU1781 (D39 *cps*$^+$ *rpsL1*) cells at an OD_{620} of 0.2 was 0.011 μmol/mg of protein extract. This amount corresponds to an estimated cellular concentration of ≈3 mM AcP. The experimental error of the AcP determinations was ≈5%.

above; see also Table S1 in the supplemental material). Like the Δ*spxB* Δ*pta* mutant, the triple mutant grew comparably to the parent strain (Fig. 3 and data not shown), even though it produced 50% of the normal ATP amount and contained negligible AcP (Table 1, row 8).

Consideration of these amounts of ATP and AcP suggests that a Δ*ackA* deletion initially decreases the cellular ATP amount by ≈50% and increases AcP amounts. Therefore, the reason Δ*ackA* mutants need to accumulate *spxB* or *spxR* suppressor mutations may be to reduce the H_2O_2 level in response to the lower cellular ATP amount, or to reduce high AcP amounts that are somehow deleterious, or both. Addition of acetate to the parent and the Δ*pta* mutant increased the cellular AcP amount by ≈1.5-fold without changing the ATP level (Table 2, rows 2 and 5). Plating the parent and Δ*pta* mutant on BA plates containing acetate at 15 mM and higher concentrations did not cause colony heterogeneity indicative of suppressor accumulation (data not shown). Therefore, modest increases in AcP amounts did not appear deleterious to cells, although we were unable to increase cellular AcP amounts above this range by adding more potassium acetate (data not shown).

In addition, we attempted to deplete AckA expression and then follow the effects on the ATP and AcP pools. As described above, expression of an ectopic copy of *ackA*$^+$ under the control of a fucose-inducible promoter complemented the Δ*ackA* mutation on BA plates containing fucose (strain IU4493 [Δ*ackA* CEP::P_{fcsK}-*ackA*$^+$]) (see Table S1 in the supplemental material). We tested whether we could also deplete AckA sufficiently in strain IU4493 in BHI broth. Cells were grown in relatively low amounts of fucose (0.2% [wt/vol]), washed, and resuspended at a low density (OD_{620}, 0.005) in BHI broth lacking or containing fucose. However, cultures lacking or containing fucose after the shift grew similarly (data not shown). Either it was not possible to sufficiently deplete the accumulated AckA amount and activity within the time frame of these growth experiments, or more likely, the P_{fcsK} promoter was leakier in cells grown in BHI broth than those on BA plates. Regardless, we were unable to obtain conclusive data about the extent of AcP accumulation following depletion of AckA before suppressor accumulation.

Effects of the SpxB-Pta-AckA pathway on TCS expression. Previously, we reported that Δ*spxB* mutants growing exponentially caused a limited number of modest changes in relative transcript amounts compared to the *spxB*$^+$ parent, even though relative AcP amount and H_2O_2 production were reduced by 80% and 90%, respectively (Table 2, row 3) (40, 42). In particular, there were no large changes in the transcription patterns of known TCS regulons (42). However, we could not rule out a role for AcP in TCS regulation, because the cellular concentration of AcP was unknown, and we had not reduced it to a negligible level (42). We used the strains described above to perform an epistasis analysis, comparing the global transcription patterns of the Δ*spxB*, Δ*spxB* Δ*ackA*, Δ*spxB* Δ*pta*, and Δ*spxB* Δ*ackA* Δ*pta* mutants (Table 3; see also Tables S3 to S6 in the supplemental material and the information in the GEO database under accession number GSE23404) (a rationale for such work was reported in reference 54). These results confirmed our previous data, showing that the Δ*spxB* mutation does not strongly affect relative transcript amounts in exponentially growing cells (Table 3, IU2173). Unexpectedly, the changes in relative transcript amounts of the Δ*spxB* Δ*ackA* Δ*pta* mutant, which produced 50% ATP and negligible AcP compared to its parent (Table 2, row 8), were largely confined to the $WalRK_{Spn}$, $CiaRH_{Spn}$, and $LiaSR_{Spn}$ TCS regulons (see Table S6 in the supplemental material). Relative transcript levels of some of the more strongly responsive regulon genes changed the most, especially in the $CiaRH_{Spn}$ regulon (Table 3, IU2837). This result shows that the function of the SpxB-Pta-AckA pathway influences the expression of only a limited number (3/13) of the complete TCSs in *S. pneumoniae*.

Of these three TCSs affected, only the $WalRK_{Spn}$ TCS regulon had changes in expression correlated with the AcP amount. The Δ*spxB* Δ*pta* mutant produced similar amounts of AcP and ATP as the triple Δ*spxB* Δ*ackA* Δ*pta* mutant (Table 3). The

TABLE 3. Microarray analysis of transcripts strongly regulated by the WalRK$_{Spn}$, CiaRH$_{Spn}$, or LiaSR$_{Spn}$ TCS in SpxB-Pta-AckA pathway mutants, compared to the D39 *spxB*$^+$ *pta*$^+$ *ackA*$^+$ parent strain

Regulon and gene tag (spd no./ spr no.)[a]	Metabolite or gene description	Relative metabolite or transcript fold change[b] in strain (genotype)							
		IU2687 (Δ*pta*)	IU2173 (Δ*spxB*)	IU3590 (Δ*spxB* Δ*ackA*)	IU2689 (Δ*spxB* Δ*pta*)	IU2837 (Δ*spxB* Δ*ackA* Δ*pta*)	IU1885 (Δ*walK*$_{Spn}$)	IU4319 (Δ*spxB* Δ*ackA* Δ*walK*$_{Spn}$)	IU3107 (Δ*spxB* Δ*pta* Δ*ackA* Δ*walK*$_{Spn}$)
	ATP	1.1 ± 0.1	1.0 ± 0.1	0.53 ± 0.04	0.50 ± 0.05	0.54 ± 0.09	ND	ND	ND
	AcP	1.0 ± 0.1	0.18 ± 0.02	1.9 ± 0.2	0.08 ± 0.04	0.07 ± 0.01	ND	ND	ND
WalRK$_{Spn}$ regulon[c]									
0104/0096	LysM domain protein	1.0	1.2	1.1	−2.2 ± 0.5	−2.5 ± 0.2	−3.2 ± 0.1	−2.0	−4.4 ± 0.9
1874/1875	LysM domain protein (putative lysozyme)	−1.1	−1.2	1.1	−3.4 ± 0.7	−2.9 ± 0.3	−7.8 ± 1.5	−7.2	−10.0 ± 1.4
2043/2021	*pcsB*; cell division protein	1.0	1.1	1.1	−1.3	−1.9 ± 0.1	−4.1 ± 0.7	−2.1	−3.9 ± 0.7
CiaRH$_{Spn}$ regulon[c]									
0775/0782	Conserved hypothetical protein	−1.2	−1.9 ± 0.4	−2.2 ± 0.8	−2.0 ± 0.7	−4.8 ± 0.4	1.7	−1.1	−1.6
0913/0931	Conserved hypothetical protein	−1.0	−2.0 ± 0.4	−3.7 ± 1.2	−3.1 ± 0.1	−7.8 ± 1.5	1.4	−1.1	−2.0 ± 0.8
2068/2045	*htrA*; serine protease	−1.0	−2.2 ± 0.5	−3.5 ± 1.6	−3.1 ± 0.6	−9.4 ± 1.9	−1.0	−1.5	−2.5 ± 0.5
LiaSR$_{Spn}$ regulon[c]									
0178/0173	Conserved hypothetical protein	1.2	1.1	−1.1	−1.2	−1.6	1.1	1.2	1.1
0351/0343	*liaS*; sensor histidine kinase	−1.0	−1.4	−1.2	−1.2	−2.2 ± 0.3	−1.2	−1.1	−1.1
0803/0810	Conserved hypothetical protein	1.1	−1.2	−1.3	−1.6	−2.5 ± 0.3	1.2	1.0	1.0

[a] Gene tags are shown for both the D39 serovar 2 strain (*spd* no.) used in the study and laboratory strain R6 (*spr* no.) used in previous studies by various laboratories.
[b] All amounts are relative to those in parent strain IU1781 (D39 *cps*$^+$ *rpsL1*). ATP and AcP values are restated from Table 2 for ease of comparison. ND, not determined.
[c] Microarray analyses were performed as described in Materials and Methods. At least three biological replicates were performed for IU2687 (Δ*pta*) and IU2837 (Δ*spxB* Δ*ackA* Δ*pta*). Two biological replicates were performed for the other strains, except IU4319 (Δ*spxB* Δ*ackA* Δ*walK*$_{Spn}$), which was evaluated once for comparison. Standard errors are indicated for fold changes above ±1.8, which was used as the cutoff. Relative transcript amounts of other WalRK$_{Spn}$, CiaRH$_{Spn}$, and LiaSR$_{Spn}$ regulon members also changed significantly but are not shown here for the sake of simplicity. Lists of all significant changes in relative transcript amounts are provided in the supplemental material and in the GEO database (accession number GSE23404).

changes in the relative transcript amounts of genes encoding the two LysM domain proteins in the WalRK$_{Spn}$ regulon were similar in the double and triple mutants. Notably, the relative transcript amounts of the WalRK$_{Spn}$ regulon genes were restored to the parent level in the Δ*spxB* Δ*ackA* mutant, which still produced a lower ATP amount, but had a modestly increased amount of AcP compared to the parent (Table 3, IU3590). We compared the effects of eliminating the WalK$_{Spn}$ histidine kinase with the modest changes in WalRK$_{Spn}$ regulon expression observed in the SpxB-Pta-AckA pathway mutants. Decreases in relative amounts of WalRK$_{Spn}$ regulon transcripts were greater in the Δ*walK*$_{Spn}$ mutant (Table 3, IU1885) than in the SpxB-Pta-AckA pathway mutants (Table 3, IU2837). Elimination of both WalK$_{Spn}$ and the SpxB-Pta-AckA pathway resulted in an approximately additive decrease (Table 3, IU3107), consistent with the interpretation that WalK$_{Spn}$ kinase activity and AcP can contribute to WalR$_{Spn}$ phosphorylation. However, this effect of AcP was only detected when AcP amounts were reduced to negligible levels, since increasing AcP amount when WalK$_{Spn}$ was absent did not significantly increase WalRK$_{Spn}$ regulon expression (Table 3, IU4319), despite the absence of the WalK$_{Spn}$ phosphatase activity for WalR$_{Spn}$~P (16).

Similar to the WalRK$_{Spn}$ TCS regulon, expression levels of the CiaRH$_{Spn}$ and LiaSR$_{Spn}$ TCS regulons were reduced strongly or weakly, respectively, by elimination of the SpxB-Pta-AckA pathway (Table 3, IU2837). In contrast to the WalRK$_{Spn}$ regulon, expression of the CiaRH$_{Spn}$ regulon was marginally reduced in the Δ*spxB* mutant, which synthesizes only 20% of the AcP of the parent strain (Table 3, IU2173). However, the epistasis analysis described above failed to show a correlation between AcP amount and CiaRH$_{Spn}$ regulon expression (Table 3). Absence of the WalK$_{Spn}$ histidine kinase did not significantly affect expression of the CiaRH$_{Spn}$ and LiaSR$_{Spn}$ regulons (Table 3, IU1885), consistent with minimal or no cross talk. But elimination of both WalK$_{Spn}$ and the SpxB-Pta-AckA pathway produced less reduction in CiaRH$_{Spn}$ regulon expression than elimination of the SpxB-Pta-AckA pathway alone (Table 3, IU2837 and IU3107). Together, these results imply that transcription levels of the CiaRH$_{Spn}$ and LiaSR$_{Spn}$ TCS regulons are influenced in complex ways by perturbations of the SpxB-Pta-AckA pathway.

DISCUSSION

In this paper, we report the first characterizations of the Pta-AckA pathway in *S. pneumoniae* and its metabolic relationship to SpxB. Both SpxB pyruvate oxidase and Pta phosphotransacetylase synthesize AcP, which can be used as an additional source of ATP in these bacteria that otherwise must synthesize ATP by substrate-level phosphorylation during glycolysis (Fig. 1). Homologs of Pta are present in most bacterial species (although Pta from Gram-positive bacteria lacks the additional amino-terminal domains present in *E. coli* Pta), but relatively few bacterial species contain SpxB, which also synthesizes H_2O_2 as a product (Fig. 1) (42). In contrast to mutations in *pta* and *spxB*, strains deleted for *ackA*, which encodes acetate kinase (Fig. 1), were unstable and accumulated sup-

pressors at a high frequency that reduced SpxB function or expression (Table 1), including inactivation of *spxR*, which encodes a positive regulator of *spxB* and *strH* (glycoprotein exoglycosidase) transcription that we identified previously (42).

This collection of mutants defective in different parts of the SpxB-Pta-AckA pathway revealed some unanticipated properties of ATP and AcP biosynthesis in *S. pneumoniae.* Cellular ATP amounts were maintained at constant levels in Δ*spxB* and Δ*pta* mutants, and also upon acetate addition to medium, which increased the AcP amount by ≈1.6-fold (Table 2). Notably, Δ*spxB* mutants contained the same amount of ATP as the parent strain. This comparison was not made in a previous study (40), which did show an 80% reduction in AcP amount in *spxB* mutants similar to that reported here (Table 2). Our results suggest that in the absence of SpxB, AcP synthesized by Pta is consumed, but not replenished, to maintain the cellular ATP pool.

In suppressed Δ*spxB* Δ*ackA* mutants or in a Δ*spxB* Δ*pta* mutant, the cellular ATP amount dropped to 50% of the wild-type level, and in the Δ*spxB* Δ*pta* and Δ*spxB* Δ*pta* Δ*ackA* mutants, the AcP amount dropped to a negligible level, although a small (≈7%) residual amount was always detected (Table 2). Surprisingly, these drastic drops in the ATP and AcP energy pools did not detectably impede the growth of mutants in BHI broth or on BA plates (Fig. 3). The cellular concentrations of ATP and AcP were estimated at ≈2 mM and ≈3 mM, respectively, in exponentially growing serotype 2 strain D39 (Table 2). Several estimates of the pneumococcal ATP pool, ranging from ≈0.3 mM to ≈6 mM, have been reported, although most reports did not provide details of how the cellular amounts were calculated. Our estimate of 2 mM most closely matches the 1 mM estimate reported in reference 49. The cellular ATP pools of *S. pneumoniae* D39 (≈2 mM [Table 2]) and *E. coli* K-12 (≈3 mM [6, 25]) were comparable in exponentially growing bacteria. Although *E. coli* has a greater capacity to synthesize ATP, it also contains nearly twice as many genes and forms cells at least twice as large as *S. pneumoniae* (3, 28). Likewise, the steady-state cellular pool of AcP in *S. pneumoniae* (≈3 mM) (Table 2) was comparable to that of *E. coli* under some growth conditions (≈3 mM) (25, 54). Thus, during exponential growth, *S. pneumoniae* reserves a remarkable amount of phosphate bond energy in AcP, which is synthesized by a pyruvate oxidase activity not present in *E. coli* and many other bacterial species (Fig. 1). An important implication from the combined results in this paper is that AcP seems to be a major energy reservoir for ATP synthesis in pneumococcus, rather than a signaling conduit between metabolic state and TCS regulation.

The accumulation of suppressors was high in Δ*ackA* mutants, which formed very small, unstable colonies under aerobic growth conditions. Every time a small, single Δ*ackA* colony was streaked, multiple large mucoid and medium-sized rough colony types were obtained, and all suppressor mutants contained mutations in *spxB* or *spxR* that reduced SpxB function or expression (Table 1; Fig. 2). In addition, the medium-sized rough colonies contained mutations in the *cps2E* or *cps2C* genes that halted capsule biosynthesis (Table 1). Genetic reconstruction experiments demonstrated that Δ*spxB* or *spxR*::Mariner mutations were necessary and sufficient to stabilize Δ*ackA* mutants, whereas Δ*cps2A′*-Δ*cps2H′* and *cps2E* (ΔA) mutations were not (see Results). Therefore, the *cps2E* and *cps2C* mutations likely occurred first in the medium-sized rough Δ*ackA* mutants, perhaps to reduce the considerable ATP load of capsule biosynthesis, but loss of capsule was not sufficient to relieve the metabolic stress caused by Δ*ackA* deletion, which further requires reduced SpxB function or expression.

The mutations that accumulated in *cps2E*, *cps2C*, *spxB*, and *spxR* in independently isolated, spontaneous Δ*ackA* suppressor strains fell into a limited set of changes that perhaps is indicative of a mutational stress response. Except for one C→T change, the eight other sequenced *cps2E* and *cps2C* mutants contained frameshift mutations involving an insertion or deletion of a single base. Of these eight frameshift mutations, three were caused by a ΔA deletion in a single run of 7 A residues in *cps2E* (Table 1). However, the other five frameshift mutations were not in runs of bases characteristic of a phase variation mechanism (34). On the other hand, we found that the *cps2E* (ΔA) could shift back to the in-frame 7-A run if bacteria were subjected to strong selection for capsule production in an animal model of infection (K. J. Wayne, unpublished results). In addition, one *spxB* and one *spxR* frameshift mutation were recovered among the seven *spxB* and *spxR* suppressor mutants (Table 1). The other five *spxB* mutations were single nucleotide changes, four of which were changes of G to other bases, including two G→T mutations, consistent with oxidative damage of G to 8-oxo-G (32). Finally, preliminary experiments using a newly constructed frameshift indicator strain suggested that the Δ*ackA* mutants accumulated most of these suppressor mutations on the selection plates following transformation (data not shown), which is again consistent with a highly stressed state that would increase frameshifts and base damage.

We considered two nonexclusive explanations as to why Δ*ackA* mutants need to reduce or eliminate SpxB function. $AckA_{Spn}$ is homologous to canonical $AckA_{Eco}$ over its whole length (data not shown), and the instability of $\Delta ackA_{Spn}$ mutants is likely caused by a metabolic pathway block, rather than some unprecedented essential interaction between AckA and another protein that does not occur in *E. coli*. The Δ*ackA* block should decrease ATP production and increase AcP amounts (Fig. 1). Reduced SpxB expression decreases H_2O_2 and AcP production (Table 2; Fig. 2). Therefore, according to one scenario, the reduced *spxB* expression simply decreases highly toxic levels of AcP back to levels that are tolerated. According to the other scenario, resistance to the high endogenous levels of H_2O_2 produced by SpxB is an energy-dependent process that requires wild-type ATP levels.

Several observations tend to support the energy dependence hypothesis, but none is definitive. The reaction catalyzed by Pta is usually reversible (Fig. 1), so high levels of AcP could be reduced by funneling it back toward acetyl-CoA and other metabolites in a Δ*ackA* mutant. But disruptions in the acetyl-CoA pathway itself could be deleterious, because of its essential role in the biosynthesis of fatty acids and other key metabolites (Fig. 1). Acetate addition led to modest increases of AcP levels in $spxB^+$ strains (Table 2) and did not result in *spxB* suppressor accumulation, as was observed for Δ*ackA* mutants. But, we were limited in how much we could increase the AcP amount by this approach. Attempts to downshift AckA expression were not successful in liquid medium, probably because of

leakiness of the fucose-regulated P_{fcsK} promoter. Elsewhere, we have demonstrated that several essential genes are required for resistance to the endogenous H_2O_2 synthesized by SpxB, and different genes are used to cope with endogenously produced and exogenously added H_2O_2 (unpublished data). The protein encoded by one of these genes consumes energy as part of its metabolic activity. Moreover, recent work has implicated the pentose phosphate shunt, which consumes NADPH, in resistance mechanisms against H_2O_2 (39). Together, these observations are consistent with the idea that a sufficient ATP level needs to be maintained for resistance to the endogenous H_2O_2 synthesized by SpxB.

Finally, this set of mutants (Table 2) allowed us to analyze effects of the SpxB-Pta-AckA pathway and AcP amount on TCS regulation patterns in *S. pneumoniae* (Table 3; see also the supplemental material). AcP phosphorylation of some response regulators plays important roles in the signaling pathways of several TCSs in *E. coli* and other bacterial species (reviewed in references 39, 53, and 54). In *S. pneumoniae*, the $WalR_{Spn}$ (VicR) response regulator is essential, whereas the $WalK_{Spn}$ (VicK) histidine kinase is not essential under standard growth conditions (16, 37, 52). One hypothesis proposed to explain this nonessentiality of $WalK_{Spn}$ is cross talk phosphorylation of $WalR_{Spn}$ by AcP, which occurs at high (≈10 mM) AcP concentrations in purified biochemical reactions over extended times (16, 38). In addition, it has been proposed that the AcP produced by SpxB generally phosphorylates response regulators (27, 45).

Previously, we reported that the 80% reduction in AcP that occurs in Δ*spxB* mutants (Table 2) (40) did not lead to large changes in transcription patterns indicative of altered TCS regulation (42). The most conspicuous change in the Δ*spxB* mutant was a small decrease near the microarray cutoff value in the relative transcript amount of the $CiaRH_{Spn}$ TCS regulon (Table 3). We also did not detect small decreases in the relative amounts of *fab* gene transcripts, as recently reported in reference 4. Complete disruption of the SpxB-Pta-AckA pathway in a triple mutant led to a negligible amount of AcP and 50% of the cellular ATP amount (Table 2). Surprisingly, these reductions did not significantly affect growth under the condition tested (Fig. 3) and resulted in a limited global transcription response that strongly decreased expression of the CiaRH TCS regulon and to a lesser extent that of the $WalRK_{Spn}$ and $LiaSR_{Spn}$ regulons (Table 3; see also Table S6 in the supplemental material).

Epistasis analysis using combinations of SpxB-Pta-AckA pathway mutations showed that expression of the $WalRK_{Spn}$ regulon was correlated with AcP amounts, but the decreases in expression levels were small (Table 3) and approximately additive, with the larger decreases in $WalRK_{Spn}$ regulon expression caused by the absence of the $WalK_{Spn}$ histidine kinase (Table 3). However, these effects only became detectable at negligible AcP amounts, which are unlikely to occur under normal physiological conditions, especially given the central role described here for AcP as an energy reservoir in *S. pneumoniae*. Likewise, at least an 80% reduction of cellular AcP amount was required to detect a marginal decrease in $CiaRH_{Spn}$ TCS regulon expression (Table 3) (42). These combined results do not support phosphorylation of pneumococcal response regulators by AcP as a general signaling mechanism, despite a relatively high (≈3 mM) estimated cellular AcP concentration (Table 2). On the other hand, normal function of the SpxB-Pta-AckA pathway quite specifically influences the expression of the three TCS regulons that mediate cell wall homeostasis and stress (reviewed in references 10 and 22). In particular, the response of the $CiaRH_{Spn}$ TCS regulon is complex (Table 3) and may reflect changes in cell wall biosynthesis that occur when the SpxB-Pta-AckA pathway is perturbed or changes in other key metabolic processes, such as protein acetylation, that are linked to this pathway (53, 54).

ACKNOWLEDGMENTS

We thank Tiffany Tsui, Alina Gutu, and Kyle Wayne for comments, discussions, and some bacterial strains and PCR amplicons used in this paper and Linda Kenney (UIC) for critical comments.

This project was supported by grant number AI060744 (to M.E.W.) from the National Institute of Allergy and Infectious Diseases. S.R.-M. was a predoctoral trainee on NIH training grant T32GM007757.

The contents of this paper are solely the responsibility of the authors and do not necessarily represent the official views of the National Institutes of Health.

REFERENCES

1. **Allegrucci, M., and K. Sauer.** 2008. Formation of *Streptococcus pneumoniae* non-phase-variable colony variants is due to increased mutation frequency present under biofilm growth conditions. J. Bacteriol. **190:**6330–6339.
2. **Auzat, I., S. Chapuy-Regaud, G. Le Bras, D. Dos Santos, A. D. Ogunniyi, I. Le Thomas, J. R. Garel, J. C. Paton, and M. C. Trombe.** 1999. The NADH oxidase of *Streptococcus pneumoniae*: its involvement in competence and virulence. Mol. Microbiol. **34:**1018–1028.
3. **Barendt, S. M., A. D. Land, L. T. Sham, W. L. Ng, H. C. Tsui, R. J. Arnold, and M. E. Winkler.** 2009. Influences of capsule on cell shape and chain formation of wild-type and *pcsB* mutants of serotype 2 *Streptococcus pneumoniae*. J. Bacteriol. **191:**3024–3040.
4. **Benisty, R., A. Y. Cohen, A. Feldman, Z. Cohen, and N. Porat.** 2010. Endogenous H(2)O(2) produced by *Streptococcus pneumoniae* controls FabF activity. Biochim. Biophys. Acta **1801:**1098–1104.
5. **Bortoni, M. E., V. S. Terra, J. Hinds, P. W. Andrew, and H. Yesilkaya.** 2009. The pneumococcal response to oxidative stress includes a role for Rgg. Microbiology **155:**4123–4134.
6. **Buckstein, M. H., J. He, and H. Rubin.** 2008. Characterization of nucleotide pools as a function of physiological state in *Escherichia coli*. J. Bacteriol. **190:**718–726.
7. **Cabre, M.** 2009. Pneumonia in the elderly. Curr. Opin. Pulm. Med. **15:**223–229.
8. **Cartee, R. T., W. T. Forsee, M. H. Bender, K. D. Ambrose, and J. Yother.** 2005. CpsE from type 2 *Streptococcus pneumoniae* catalyzes the reversible addition of glucose-1-phosphate to a polyprenyl phosphate acceptor, initiating type 2 capsule repeat unit formation. J. Bacteriol. **187:**7425–7433.
9. **Crook, D. W., A. B. Brueggemann, K. L. Sleeman, and T. E. A. Peto.** 2004. Pneumococcal carriage, p. 136–147. *In* E. I. Tuomanen, T. J. Mitchell, D. A. Morrison, and B. G. Spratt (ed.), The pneumococcus. ASM Press, Washington, DC.
10. **Dubrac, S., P. Bisicchia, K. M. Devine, and T. Msadek.** 2008. A matter of life and death: cell wall homeostasis and the WalKR (YycGF) essential signal transduction pathway. Mol. Microbiol. **70:**1307–1322.
11. **El-Mansi, M., A. J. Cozzone, J. Shiloach, and B. J. Eikmanns.** 2006. Control of carbon flux through enzymes of central and intermediary metabolism during growth of *Escherichia coli* on acetate. Curr. Opin. Microbiol. **9:**173–179.
12. **Felmingham, D., R. Canton, and S. G. Jenkins.** 2007. Regional trends in beta-lactam, macrolide, fluoroquinolone and telithromycin resistance among *Streptococcus pneumoniae* isolates 2001–2004. J. Infect. **55:**111–118.
13. **Fredericks, C. E., S. Shibata, S. Aizawa, S. A. Reimann, and A. J. Wolfe.** 2006. Acetyl phosphate-sensitive regulation of flagellar biogenesis and capsular biosynthesis depends on the Rcs phosphorelay. Mol. Microbiol. **61:**734–747.
14. **Gottshalk, G.** 1986. Bacterial metabolism, 2nd ed. Springer-Verlag, New York, NY.
15. **Gueriri, I., S. Bay, S. Dubrac, C. Cyncynatus, and T. Msadek.** 2008. The Pta-AckA pathway controlling acetyl phosphate levels and the phosphorylation state of the DegU orphan response regulator both play a role in regulating *Listeria monocytogenes* motility and chemotaxis. Mol. Microbiol. **70:**1342–1357.
16. **Gutu, A. D., K. J. Wayne, L. T. Sham, and M. E. Winkler.** 2010. Kinetic

characterization of the WalRKSpn (VicRK) two-component system of *Streptococcus pneumoniae*: dependence of WalKSpn (VicK) phosphatase activity on its PAS domain. J. Bacteriol. **192:**2346–2358.
17. **Hendriksen, W. T., H. J. Bootsma, S. Estevao, T. Hoogenboezem, A. de Jong, R. de Groot, O. P. Kuipers, and P. W. Hermans.** 2008. CodY of *Streptococcus pneumoniae*: link between nutritional gene regulation and colonization. J. Bacteriol. **190:**590–601.
18. **Hendriksen, W. T., T. G. Kloosterman, H. J. Bootsma, S. Estevao, R. de Groot, O. P. Kuipers, and P. W. Hermans.** 2008. Site-specific contributions of glutamine-dependent regulator GlnR and GlnR-regulated genes to virulence of *Streptococcus pneumoniae*. Infect. Immun. **76:**1230–1238.
19. **Henriques-Normark, B., and S. Normark.** 2010. Commensal pathogens, with a focus on *Streptococcus pneumoniae*, and interactions with the human host. Exp. Cell Res. **316:**1408–1414.
20. **Hoskins, J., W. E. Alborn, Jr., J. Arnold, L. C. Blaszczak, S. Burgett, B. S. DeHoff, S. T. Estrem, L. Fritz, D. J. Fu, W. Fuller, C. Geringer, R. Gilmour, J. S. Glass, H. Khoja, A. R. Kraft, R. E. Lagace, D. J. LeBlanc, L. N. Lee, E. J. Lefkowitz, J. Lu, P. Matsushima, S. M. McAhren, M. McHenney, K. McLeaster, C. W. Mundy, T. I. Nicas, F. H. Norris, M. O'Gara, R. B. Peery, G. T. Robertson, P. Rockey, P. M. Sun, M. E. Winkler, Y. Yang, M. Young-Bellido, G. Zhao, C. A. Zook, R. H. Baltz, S. R. Jaskunas, P. R. Rosteck, Jr., P. L. Skatrud, and J. I. Glass.** 2001. Genome of the bacterium *Streptococcus pneumoniae* strain R6. J. Bacteriol. **183:**5709–5717.
21. **Iyer, R., N. S. Baliga, and A. Camilli.** 2005. Catabolite control protein A (CcpA) contributes to virulence and regulation of sugar metabolism in *Streptococcus pneumoniae*. J. Bacteriol. **187:**8340–8349.
22. **Jordan, S., M. I. Hutchings, and T. Mascher.** 2008. Cell envelope stress response in Gram-positive bacteria. FEMS Microbiol. Rev. **32:**107–146.
23. **Kadioglu, A., J. N. Weiser, J. C. Paton, and P. W. Andrew.** 2008. The role of *Streptococcus pneumoniae* virulence factors in host respiratory colonization and disease. Nat. Rev. Microbiol. **6:**288–301.
24. **Kazmierczak, K. M., K. J. Wayne, A. Rechtsteiner, and M. E. Winkler.** 2009. Roles of *rel* in stringent response, global regulation and virulence of serotype 2 S*treptococcus pneumoniae* D39. Mol. Microbiol. **72:**590–611.
25. **Klein, A. H., A. Shulla, S. A. Reimann, D. H. Keating, and A. J. Wolfe.** 2007. The intracellular concentration of acetyl phosphate in *Escherichia coli* is sufficient for direct phosphorylation of two-component response regulators. J. Bacteriol. **189:**5574–5581.
26. **Kreth, J., H. Vu, Y. Zhang, and M. C. Herzberg.** 2009. Characterization of hydrogen peroxide-induced DNA release by *Streptococcus sanguinis* and *Streptococcus gordonii*. J. Bacteriol. **191:**6281–6291.
27. **Kuboniwa, M., G. D. Tribble, C. E. James, A. O. Kilic, L. Tao, M. C. Herzberg, S. Shizukuishi, and R. J. Lamont.** 2006. *Streptococcus gordonii* utilizes several distinct gene functions to recruit *Porphyromonas gingivalis* into a mixed community. Mol. Microbiol. **60:**121–139.
28. **Lanie, J. A., W. L. Ng, K. M. Kazmierczak, T. M. Andrzejewski, T. M. Davidsen, K. J. Wayne, H. Tettelin, J. I. Glass, and M. E. Winkler.** 2007. Genome sequence of Avery's virulent serotype 2 strain D39 of *Streptococcus pneumoniae* and comparison with that of unencapsulated laboratory strain R6. J. Bacteriol. **189:**38–51.
29. **Lynch, J. P., III, and G. G. Zhanel.** 2010. *Streptococcus pneumoniae*: epidemiology and risk factors, evolution of antimicrobial resistance, and impact of vaccines. Curr. Opin. Pulm. Med. **16:**217–225.
30. **Madeddu, G., M. Laura Fiori, and M. Stella Mura.** 2010. Bacterial community-acquired pneumonia in HIV-infected patients. Curr. Opin. Pulm. Med. **16:**201–207.
31. **Merritt, J., F. Qi, and W. Shi.** 2005. A unique nine-gene *comY* operon in *Streptococcus mutans*. Microbiology **151:**157–166.
32. **Michaels, M. L., and J. H. Miller.** 1992. The GO system protects organisms from the mutagenic effect of the spontaneous lesion 8-hydroxyguanine (7,8-dihydro-8-oxoguanine). J. Bacteriol. **174:**6321–6325.
33. **Moscoso, M., E. Garcia, and R. Lopez.** 2009. Pneumococcal biofilms. Int. Microbiol. **12:**77–85.
34. **Moxon, E. R., P. B. Rainey, M. A. Nowak, and R. E. Lenski.** 1994. Adaptive evolution of highly mutable loci in pathogenic bacteria. Curr. Biol. **4:**24–33.
35. **Munoz-Elias, E. J., J. Marcano, and A. Camilli.** 2008. Isolation of *Streptococcus pneumoniae* biofilm mutants and their characterization during nasopharyngeal colonization. Infect. Immun. **76:**5049–5061.
36. **Neuhard, J., and P. Nygaard.** 1987. Purines and pyrimidines, p. 445–473. *In* F. C. Neidhardt (ed.), *Escherichia coli* and *Salmonella typhimurium:* cellular and molecular biology, vol. 1. American Society for Microbiology, Washington, DC.
37. **Ng, W. L., G. T. Robertson, K. M. Kazmierczak, J. Zhao, R. Gilmour, and M. E. Winkler.** 2003. Constitutive expression of PcsB suppresses the requirement for the essential VicR (YycF) response regulator in *Streptococcus pneumoniae* R6. Mol. Microbiol. **50:**1647–1663.
38. **Ng, W. L., H. C. Tsui, and M. E. Winkler.** 2005. Regulation of the *pspA* virulence factor and essential *pcsB* murein biosynthetic genes by the phosphorylated VicR (YycF) response regulator in *Streptococcus pneumoniae*. J. Bacteriol. **187:**7444–7459.
39. **Ogunniyi, A. D., L. K. Mahdi, M. P. Jennings, A. G. McEwan, C. A. McDevitt, M. B. Van der Hoek, C. J. Bagley, P. Hoffmann, K. A. Gould, and J. C. Paton.** 2010. Central role of manganese in regulation of stress responses, physiology and metabolism in *Streptococcus pneumoniae*. J. Bacteriol. **192:**4489–4497.
40. **Pericone, C. D., S. Park, J. A. Imlay, and J. N. Weiser.** 2003. Factors contributing to hydrogen peroxide resistance in *Streptococcus pneumoniae* include pyruvate oxidase (SpxB) and avoidance of the toxic effects of the Fenton reaction. J. Bacteriol. **185:**6815–6825.
41. **Pruss, B. M., and A. J. Wolfe.** 1994. Regulation of acetyl phosphate synthesis and degradation, and the control of flagellar expression in Escherichia coli. Mol. Microbiol. **12:**973–984.
42. **Ramos-Montanez, S., H. C. Tsui, K. J. Wayne, J. L. Morris, L. E. Peters, F. Zhang, K. M. Kazmierczak, L. T. Sham, and M. E. Winkler.** 2008. Polymorphism and regulation of the *spxB* (pyruvate oxidase) virulence factor gene by a CBS-HotDog domain protein (SpxR) in serotype 2 *Streptococcus pneumoniae*. Mol. Microbiol. **67:**729–746.
43. **Robertson, G. T., W. L. Ng, J. Foley, R. Gilmour, and M. E. Winkler.** 2002. Global transcriptional analysis of *clpP* mutations of type 2 *Streptococcus pneumoniae* and their effects on physiology and virulence. J. Bacteriol. **184:**3508–3520.
44. **Somerville, G. A., and R. A. Proctor.** 2009. At the crossroads of bacterial metabolism and virulence factor synthesis in staphylococci. Microbiol. Mol. Biol. Rev. **73:**233–248.
45. **Spellerberg, B., D. R. Cundell, J. Sandros, B. J. Pearce, I. Idanpaan-Heikkila, C. Rosenow, and H. R. Masure.** 1996. Pyruvate oxidase, as a determinant of virulence in *Streptococcus pneumoniae*. Mol. Microbiol. **19:**803–813.
46. **Sung, C. K., H. Li, J. P. Claverys, and D. A. Morrison.** 2001. An *rpsL* cassette, janus, for gene replacement through negative selection in *Streptococcus pneumoniae*. Appl. Environ. Microbiol. **67:**5190–5196.
47. **Taniai, H., K. Iida, M. Seki, M. Saito, S. Shiota, H. Nakayama, and S. Yoshida.** 2008. Concerted action of lactate oxidase and pyruvate oxidase in aerobic growth of *Streptococcus pneumoniae*: role of lactate as an energy source. J. Bacteriol. **190:**3572–3579.
48. **Tettelin, H., K. E. Nelson, I. T. Paulsen, J. A. Eisen, T. D. Read, S. Peterson, J. Heidelberg, R. T. DeBoy, D. H. Haft, R. J. Dodson, A. S. Durkin, M. Gwinn, J. F. Kolonay, W. C. Nelson, J. D. Peterson, L. A. Umayam, O. White, S. L. Salzberg, M. R. Lewis, D. Radune, E. Holtzapple, H. Khouri, A. M. Wolf, T. R. Utterback, C. L. Hansen, L. A. McDonald, T. V. Feldblyum, S. Angiuoli, T. Dickinson, E. K. Hickey, I. E. Holt, B. J. Loftus, F. Yang, H. O. Smith, J. C. Venter, B. A. Dougherty, D. A. Morrison, S. K. Hollingshead, and C. M. Fraser.** 2001. Complete genome sequence of a virulent isolate of *Streptococcus pneumoniae*. Science **293:**498–506.
49. **Trombe, M. C., G. Laneelle, and A. M. Sicard.** 1984. Characterization of a *Streptococcus pneumoniae* mutant with altered electric transmembrane potential. J. Bacteriol. **158:**1109–1114.
50. **Tsui, H. C., D. Mukherjee, V. A. Ray, L. T. Sham, A. L. Feig, and M. E. Winkler.** 2010. Identification and characterization of noncoding small RNAs in *Streptococcus pneumoniae* serotype 2 strain D39. J. Bacteriol. **192:**264–279.
51. **van der Poll, T., and S. M. Opal.** 2009. Pathogenesis, treatment, and prevention of pneumococcal pneumonia. Lancet **374:**1543–1556.
52. **Winkler, M. E., and J. A. Hoch.** 2008. Essentiality, bypass, and targeting of the YycFG (VicRK) two-component regulatory system in gram-positive bacteria. J. Bacteriol. **190:**2645–2648.
53. **Wolfe, A. J.** 2005. The acetate switch. Microbiol. Mol. Biol. Rev. **69:**12–50.
54. **Wolfe, A. J.** 2010. Physiologically relevant small phosphodonors link metabolism to signal transduction. Curr. Opin. Microbiol. **13:**204–209.
55. **Xayarath, B., and J. Yother.** 2007. Mutations blocking side chain assembly, polymerization, or transport of a Wzy-dependent *Streptococcus pneumoniae* capsule are lethal in the absence of suppressor mutations and can affect polymer transfer to the cell wall. J. Bacteriol. **189:**3369–3381.
56. **Yesilkaya, H., F. Spissu, S. M. Carvalho, V. S. Terra, K. A. Homer, R. Benisty, N. Porat, A. R. Neves, and P. W. Andrew.** 2009. Pyruvate formate lyase is required for pneumococcal fermentative metabolism and virulence. Infect. Immun. **77:**5418–5427.
57. **Yother, J.** 2004. Capsules, p. 30–48. *In* E. I. Tuomanen, T. J. Mitchell, D. A. Morrison, and B. G. Spratt (ed.), The pneumococcus. ASM Press, Washington, DC.
58. **Zapun, A., T. Vernet, and M. G. Pinho.** 2008. The different shapes of cocci. FEMS Microbiol. Rev. **32:**345–360.